Lasers in Manufacturing and Materials Processing (2022) 9:81–101
https://doi.org/10.1007/s40516-022-00164-8

Fabrication of Thin Walls with and without Close Loop Control as a Function of Scan Strategy Via Direct Energy Deposition

Nashit Ali[1] · Luca Tomesani[1] · Alessandro Ascari[1] · Alessandro Fortunato[1]

Accepted: 6 January 2022 / Published online: 1 February 2022

Abstract

Direct Energy Deposition (DED) is a technique used to fabricate metallic parts and is a subcategory of metal additive manufacturing. Despite of its vast advantages over traditional manufacturing the deployment at industrial level is still limited due to underlaying concerns of process stability and repeatability. In-situ monitoring, therefore, is indispensable while depositing via DED. The present experiment is a step towards enhancing our current understanding of the DED when coupled with a closed loop control system to control melt pool width for deposition of thin-walled structures, and as a function of scan strategy. 316L stainless steel powder was deposited on S235JR substrate. A total of 6 iterations are reported, out of many performed, of which 3 were without the closed loop control. Also, to understand the effect of scan strategy as a function of laser power. Two different scan strategies were employed for understanding of the issue i.e., unidirectional, and bidirectional. Apart from the geometrical consistency of the wall, microhardness, density calculations and microstructure were investigated. The geometric consistency was found to be almost perfect with the bidirectional scan strategy. In case of unidirectional scan strategy, the wall shows a negative slope along the other extreme regardless of the closed loop control system. Dilution zone shows the hardness greater than both the substrate and the wall. The specimens fabricated without the use of closed loop control were found to be denser than their counterparts. This was found to be true also in case of manual reduction of power during each layer.

Keywords Metal Additive Manufacturing (MAM) · Direct Energy Deposition (DED) · CLAMIR · AISI 316L · Thin-Walled features

✉ Nashit Ali
nashit.ali93@gmail.com

[1] Department of Industrial Engineering (DIN), University of Bologna, Bologna, Italy

Introduction

Direct Energy Deposition (DED) is a class of Metal Additive Manufacturing (MAM) that has gained huge interest in academia as well as in industry. The reason for this interest could be justified with the huge demand of materials which are expected to perform under harsh conditions and have huge geometric constraints [1]. DED systems typically use a laser to melt the powder in the presence of an inert gas. The inert gas is used to avoid oxidation and at the same time promotes cooling. The laser power melts the powder and creates a melt pool onto the substrate that is solidified, and the process is repeated layer upon layer [2]. MAM secured its place in aerospace and biomedical applications. However, the applications of DED are limited due to lack of uniform and reliable properties [3]. Repetitive melting and remelting of successive layers (an attribute of DED) give rise to complex microstructures [4]. The geometrical features must also be maintained. Thin-walled structures are common in aerospace, automotive and many other sectors and is one of the main applications of Additive Manufacturing (AM). The fabrication of such thin-walled structures is quite challenging due to complex stress distribution [5]. Also, it is often of interest to know the smallest possible feature which is geometrically consistent to be manufactured by DED [6]. Effective control of process parameters such as scan speed, laser speed, feed rate etc. govern the overall properties of the final part. Therefore, it is essential to control these properties effectively[7].

Jichang Liu and et al. [8] studied the effects of process variables on formation of thin metallic wall and showed that the width of wall depends on the melt pool dimensions. The geometry of clad is an important process characteristic. Various studies have shown the relationship between process parameters and height of thin walls [9–14].DED involves complex thermal cycles during the build. As new layers are built the previous ones are constantly melted and remelted, thus, giving rise to this thermal complexity[15]. A linear relationship between wall height and process parameters is presented through the work of Tarik Amine and et al. [10] which can be utilized for height prediction of the part.

To address these issues process monitoring has become the hotspot of research. Geometric and temperature signatures are one of the most monitored aspects to avoid geometric distortions during the build which can even be extended to control the mechanical properties of the final build part. Thus, in situ monitoring and adaptive control enables the repeatability of DED [16].

In line monitoring is an active research area and is uniquely suitable for DED due to its layer wise build nature. Process Monitoring and Defect Detection are two main areas of in-situ monitoring. Process Monitoring involves the measurement of melt pool width (size and shape), temperature of the melt pool and plasma generated by the laser as in interacts with the melt pool. This monitoring is effective only if it is used to control the related paraments in real time [17]. Adaptive Control Technology is considered as the potential solution to solve this problem in which selected inputs are controlled in response to specific outputs. For example, geometry signatures of clad is important to control in DED to achieve a geometrically stable final part [18].

S. Molarejo [19] developed a feed forward controller with laser power as input and clad width as output signal. The known desired width for melt pool of an identified model was successfully controlled and a stable cylindrical geometry was fabricated. Laser power was controlled in real time to keep the melt pool width according to the identified desired value [19]. Yaoyu Ding and Radovan Kovacevic [20] controlled the melt pool width via controlling the powder feed rate through a sensing and control system developed for an 8-axis robotized DED system. A simple PID controller with feed forward action was developed to successfully control the melt pool width. Two L-shaped single bead walls were built with and without the closed loop control. The inconsistency in bead width, the build-ups at the end were eliminated by use of this close loop system [20]. Meysam Akbari and Radovan Kovacevic [21] also developed a closed loop control to keep the melt pool width stable. 316L thin-walled structures built in response showed that this real time control of laser power successfully maintained the melt pool width and exhibits finer microstructure as compared to the one without the control [21]. Song et al. [22] developed a hybrid control system that monitors and control the melt pool height and temperature using three triangulated cameras and a colour pyrometer to maintain the height of clad by managing laser power in real time. Vision based coaxial melt pool monitoring system was reported by Vandone et al. [23] where a visible light camera was integrated into the optical chain but resulted in noisy signals with different materials. Sörn Ocylok et al. [24] monitored the effect of main process parameters (laser power, feed rate, powder mass flow) with camera based co axial monitoring system and reported laser power to be the most influential characteristic in defining melt pool size. Vito Errico et al. [25] monitored the melt pool geometry via coaxial monitoring system and used image algorithm to depict the melt pool geometry for fabrication of thin walls using different scan strategies. The literature describes the feasibility of using various monitoring systems for fabrication of thin walls via DED. However, it does not address the effect of real time close loop control system for different scan strategies for such fabrications.

Therefore, the aim of this experimental work is to describe the closed loop control system not only as a function of laser power to control the melt pool width but also in terms of two possible scan strategies for thin wall deposition. Also, the effect of gradual power reduction on deposition of thin walls are discussed.

Experimentation

The experiments were conducted on a robotized DED system. The cladding head was mounted on a six axis ABB Robot (IRB 4600). Additional 2-axis were given by a roto tilting table (IRBP A250). A 3KW “Laser Line” Diode Laser was used. (Wavelength 980 nm) and 1 mm fibre used for its connection to the cladding head. The laser spot diameter was 2 mm onto the substrate surface with a head stand-off distance of 25 mm. The powder was delivered through a coaxial nozzle made by GTV. The nozzle was cooled via flow of water through the chiller. The system was equipped with a dual Powder Feeder (GTV), however, only one feeder was used to feed the powder to the nozzle. The closed loop control system named CLAMIR

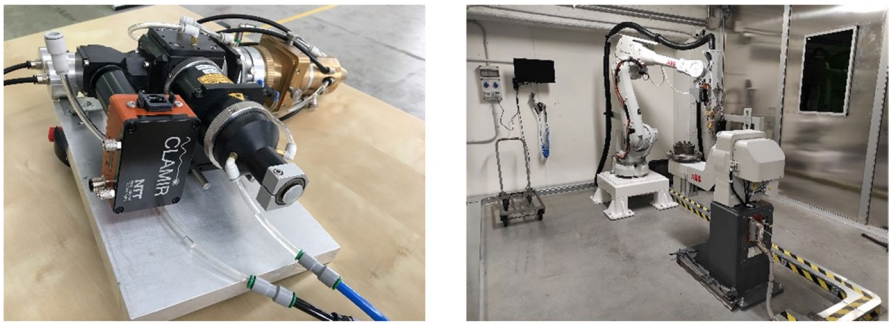

Fig. 1 (a) CLAMIR installation in cladding head (b) Machine set-up

made by New Infrared Technologies was installed into the laser optics and mounted co axially on to deposition head. CLAMIR controls the melt pool width and adjust the laser power in real time to keep the melt pool stable (Fig. 1).

AISI 316L stainless steel powder suitable for DED with a particle size ranging from 50 µm-150 µm was used. The particle size distribution for the powder is given in Table 1 and its chemical composition is reported in Table 2. The substrate choice in case of DED is generally inspired from the same class of the powder to be deposited. In this case S235JR was used as a substrate material, the dimensions of which are presented in the Table 3.

The process parameters used in this experiment were taken from the previous handling of the same powder with given DED system. The stand-off distance between the nozzle and the deposited material must be kept constant to achieve good geometric stability. The increment for each layer was selected based on the previously performed experiments. Due to the complex nature of the process, as of now, there does not exist a standard way to determine these values. Therefore, in general, this increment value on the z-axis is based on hit and trial method and a value of 0.4 mm was deemed suitable for our system and was therefore employed for this experiment.

Argon was used as carrier and shielding gas with a flow rate of 7.5 l/min and 20 l/min respectively. Scan speed and powder feed rate were kept constant at a rate

Table 1 Powder size distribution

Powder: 316L	
size	%
-53um	3.50
53-63um	2.00
63-90um	38.60
90-125um	47.30
125-150um	7.00
+150um	1.60

Table 2 Chemical composition of powder (wt.%)

Material	C	Si	Mn	P	S	N	Cr	Mo	Ni	Cu	Co	Fe
316L stainless steel	0.016	0.47	1.82	0.024	0.025	0.075	16.81	2.07	10.12	0.27	0.19	base

of 17 mm/s and 9.1 g/min respectively. A total of 70 layers were deposited for all the samples. More detailed process parameters are reported in Table 4 along with results.

The closed loop system (CLAMIR) used in the experiment was set-up with process specific parameters according to the user manual provided. More details are provided in later section. It is important to set up the parameters for CLAMIR properly as it varies from process to process.

Methodology

A RAPID code from ABB robotics was developed to fabricate the thin-walled structures. For creating simpler geometries, it was deemed to be more feasible, to use manual programming rather than a slicing software. The former statement holds as with manual programming there is more control over the deposition pattern.

The specimens were built with and without the closed loop control. All the parameters were kept constant except laser power which was controlled by CLAMIR in case of closed loop-controlled samples. Constant and gradual reduction in laser power were employed. Since the constant power mode resulted in inconsistent wall therefore manual reduction of power was employed to clearly examine the effect of scan strategy among the samples. In constant power mode the power was fed at constant rate via the controller whereas in manual power reduction mode the power was reduced via 100 W with each successive layer. This value was selected on previous handling of same powder and from viewing the data of CLAMIR but was mainly based on hit and trial approach. Two different scan strategies were used and were named as Unidirectional and Bidirectional as depicted in the Fig. 2. With unidirectional scan strategy the laser was turned off for the return path of the clad and vice versa for the bidirectional. A total of 70 layers were deposited for all the samples.

CLAMIR

The melt pool width as process variable was controlled by adjusting laser power in real time by using a closed loop-controlled system named as CLAMIR. CLAMIR was installed in the laser optics mounted onto laser head coaxially to monitor the melt pool width from the top. The control system was based on a

Table 3 Substrate dimensions

Substrate	Length (mm)	Width (mm)	Height (mm)
S235JR	80	10	10

Table 4 Table of results

Sample	Scan Strategy	Power Mode	Initial Power (W)	ΔP (W)	l (mm)	l' (mm)	h' (mm)	h" (mm)	w (mm)	w" (mm)	b (mm)	d (%)
1	Bidirectional	Constant	2000	0	40	42.01	17.24	14.53	3.27	2.7	0.803	99.78
2	Bidirectional	Manual Reduction	2000	100	40	42.06	30.95	30.21	3.2	2.6	0.798	99.66
3	Unidirectional	Manual Reduction	2000	100	40	33.01	33.01	1	2.97	2.76	0.777	99.95
4	Bidirectional	CLAMIR	2000	CLAMIR controlled	40	42.17	32.46	31.86	2.81	2.63	0.791	99.50
5	Bidirectional	CLAMIR	2000	CLAMIR controlled	40	41.8	32.27	32.26	2.52	2.22	0.258	99.40
6	Unidirectional	CLAMIR	2000	CLAMIR controlled	40	33	32.56	1.24	2.46	1.59	0.819	99.77

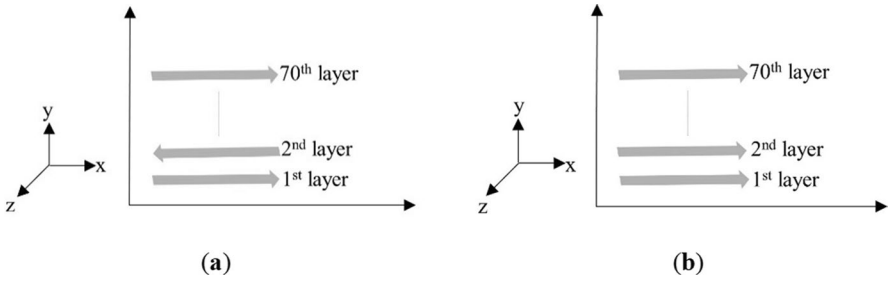

Fig. 2 Scan strategies. (a) Bi-directional (laser on from both extremes of track) (b) Uni-directional (Laser on at one extreme of track)

high-speed infrared camera that acquires images of melt pool width. These images were captured at a rate of 1 kHz and were 64 × 64 pixels. It implies that one thousand measurements of melt pool width were acquired in one second via these captured images, defined by a set threshold value. A shot taken from the visualization software provided with CLAMIR is shown in Fig. 3.

This main screen depicts the information that is being generated by the camera at given frame number. The camera was filtered for the visible range the image therefore depicts melt pool as seen by the camera. The "Track Count" on the left side is controlled by the signals of "on" and "off" as received from the laser in case of "tracks mode". It is worth noting that the "Temperature" section shows a value of 25.6 °C. This value indicates the temperature of the system and should be kept within the range of 25 °C or 26 °C.

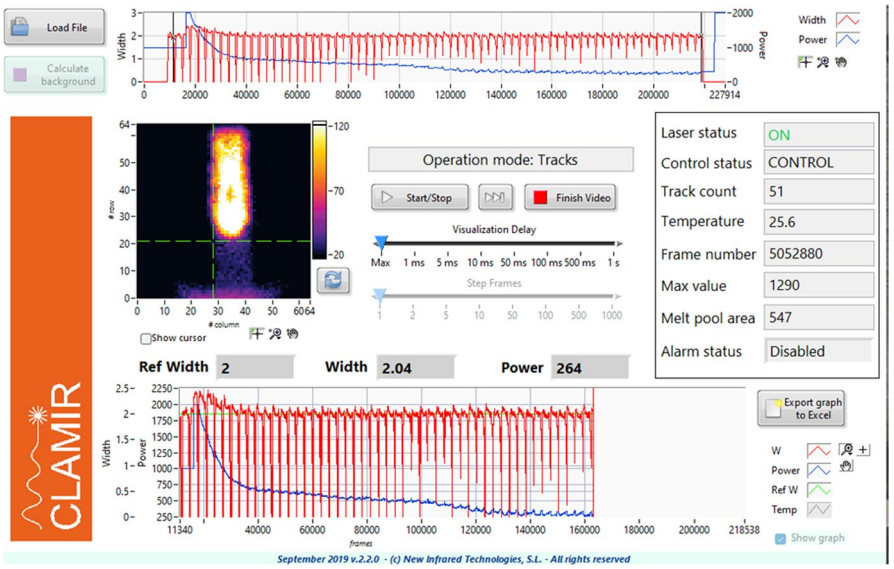

Fig. 3 CLAMIR during process control

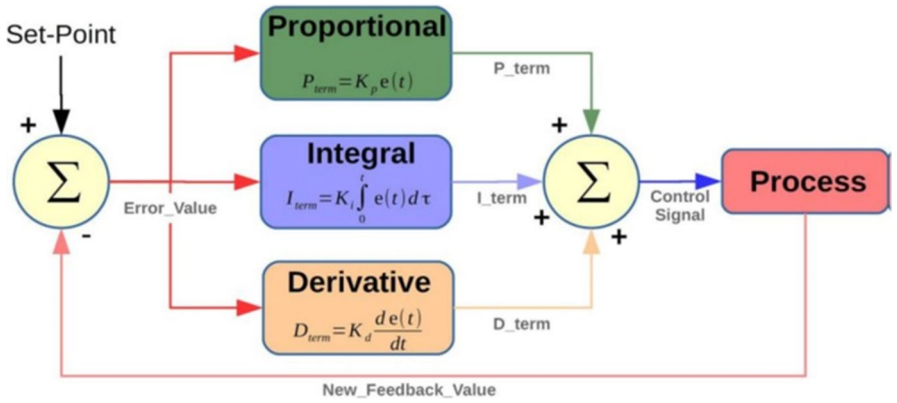

Fig. 4 CLAMIR working principle [26]

Setting-Up CLAMIR

It is important to set-up the system properly to have reasonable results. The settings mainly depend on the geometry and the material to be processed. The details of settings that are related to hardware of the system are omitted for the sake of clarity and only relevant settings are discussed.

CLAMIR had three operational modes namely "manual mode", "tracks mode" and "continuous mode". This setting was dependent upon the geometry to be built. As the name implies "manual mode" was more of a monitoring mode and operates with user set laser power. This mode was critical to investigate the melt pool width with constant laser power. The main difference between continuous and tracks mode is in laser on and laser off signals. For building thin walls "Tracks Mode" was selected. This mode performs a close loop control of laser power to keep the melt pool width constant. Figure 4 shows the operation carried out during the process.

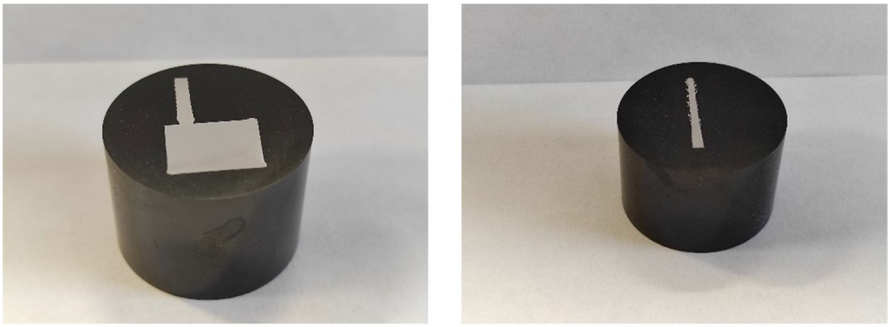

(a) **(b)**

Fig. 5 Sample profiling **(a)** bottom half of wall with substrate **(b)** top half of wall

The melt pool can be controlled depending on the data acquired during the set tracks or a manual value can be forced to be followed by the system and this value is to be inserted in a dedicated reference width box in settings in case of latter. For sample 4 in this experiment the reference width was set to be 2 mm whereas for sample 5 the melt pool width value was acquired during the deposition of first three layers and then the control started to implement width values from the fourth layer. It is worth noting that the acquired melt pool width during the first three layers accounted for 2.31 mm for sample 5.

Another important parameter to set was the "idle time" in CLAMIR. For example, in the current experiment the laser was switched off and then switched back on. It is critical to set the idle time properly so as when the laser is off during the process; system knows that it's the same process. This time was set to be 30 s for this experiment which is also the highest possible value that can be set with this system. If this time is not set properly then the system can detect it as a new process, upon returning to "laser on" from "laser off" thus start to acquire new values of melt pool width and can lead to undesirable results.

Threshold values differentiate between melt pool and the background. It is another critical value to be set properly since this will govern the area of melt pool. This value depends on the material to be processed. For the current experiment this value was set to be 1100. This value is acquired by monitoring of the process during initial trials of processing the material and adjusted accordingly for the final input for the main experiment.

Specimen Preparation

The samples were sectioned and prepared for metallurgical analysis (Fig. 5). Figure 6 shows the sectioning position for the samples. To avoid the discrepancies

Notation	Parameter
l	Theoretical length of wall
l'	Maximum length of wall
h'	Maximum height of wall
h"	Minimum height of wall
w	Maximum width of wall
w"	Minimum width of wall
b	Depth of melt pool below the substrate level
d	Density

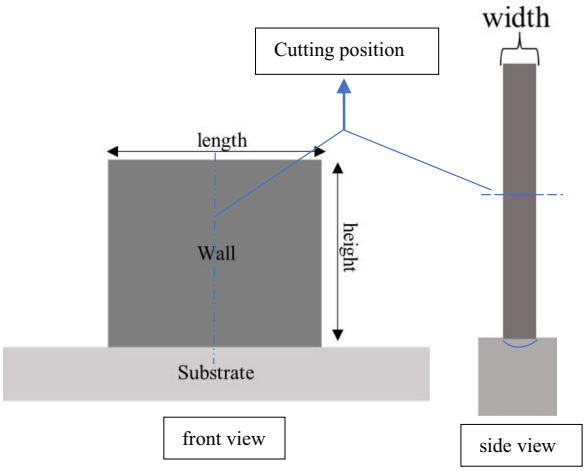

Fig. 6 Geometrical considerations along with notations used

due to acceleration and deceleration the walls were cut from the middle along the length as shown in Fig. 6. Since sample 3 and sample 6 as seen from Fig. 8 were not geometrically consistent for the height therefore these were sectioned where maximum height was achieved along the length. The wall samples were also cut into half to make the size feasible for the diameter of the mounting press moulding machine. The samples were mounted and polished with Sic abrasive paper from grit size ranging from 800 µm to 2000 µm. The samples were then polished by up to 1 µm by using diamond spray (Fig. 5). After the optical microscopy analysis, the specimens were etched using Nital etchant to reveal the deposition depth. The specimens were polished once again and etched with Villela's reagent which uncovered the microstructure.

Results and Discussion

The deposition of thin walls involves more challenging heat transfer as compared to other geometries build via DED. The following sections provide a discussion about the results obtained depending upon the scan strategy and effect of closed loop control. Figure 6 shows the schematic of wall along with the notations used for results.

Figure 7 shows all the cross-sectional images for all samples. The left side shows the bottom half of wall with substrate whereas the right side shows the top half of wall for each respective image except for sample 1. As for sample 1 the height of wall did not reach to a value above the constraint of our mounting press, therefore, was left as it is.

Table 4 depicts the measurements for all the samples along with their respective process parameters. ΔP in the table corresponds to the reduction in power during each successive layer when controlled manually and without the use of

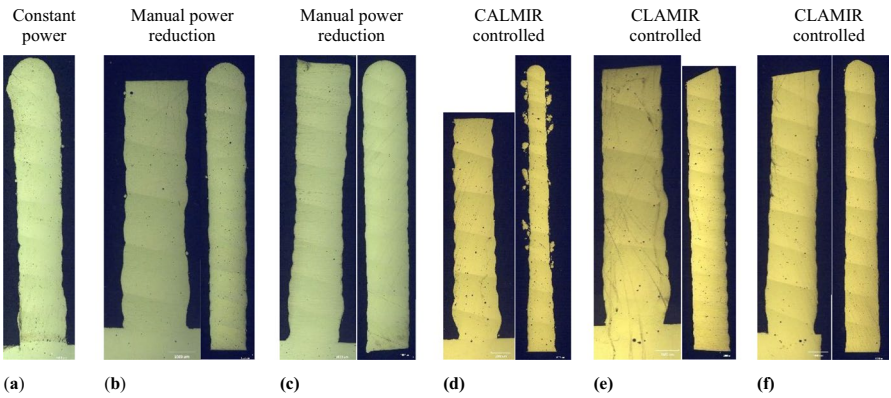

Fig. 7 Cross-sectional optical micrographs **(a)** sample 1 **(b)** sample 2 **(c)** sample 3 **(d)** sample 4 **(e)** sample 5 **(f)** sample 6

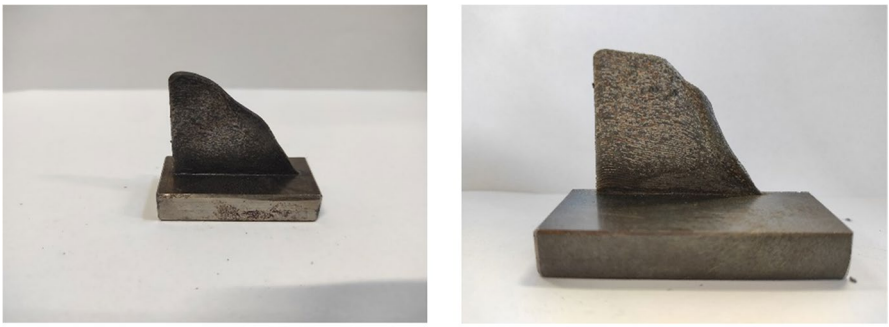

Fig. 8 **(a)** Sample 3(with manual power reduction mode) and **(b)** Sample 6 (with CLAMIR)- (unidirectional scan strategy)

CLAMIR. The successive reduction of power in case of samples fabricated via CLAMIR are shown graphically in geometric analysis section.

The initial power in above table is the power set up at the start of fabrication of each sample. This power remained constant for all 70 layers in case of constant power mode (sample 1). The power was reduced by 100 W each successive layer for manual power reduction mode (sample 2 and sample 3) and was controlled by CLAMIR for samples 4, sample 5 and sample 6. The reduction of this power in case of CLAMIR was dependent upon the settings as discussed above in CLAMIR set-up section. For instance, when CLAMIR was forced to keep the reference width at 2 mm (Sample 4) the power reduction started from the 4^{th} layer. It is important to give some time before starting the control as to let the system stabilise. For sample 5 and sample 6 CLAMIR was set to calculate the width during the first three layers and the control of power started from the fourth layer.

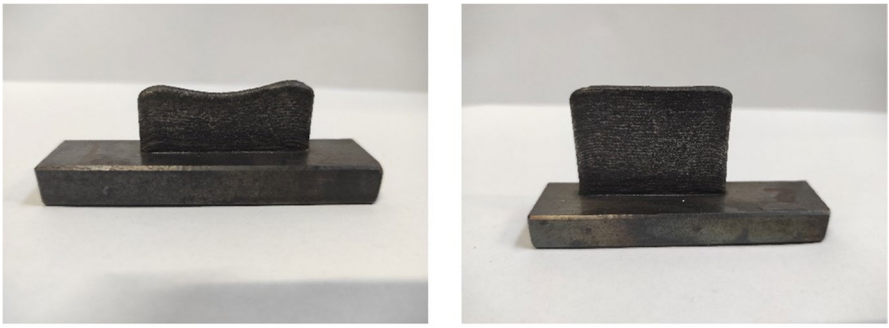

Fig. 9 **(a)** Sample 1 (constant power mode) **(b)** Sample 2 (manual power reduction mode)—Bidirectional Scan Strategy

Fig. 10 Sample 2—Variable Wall Width

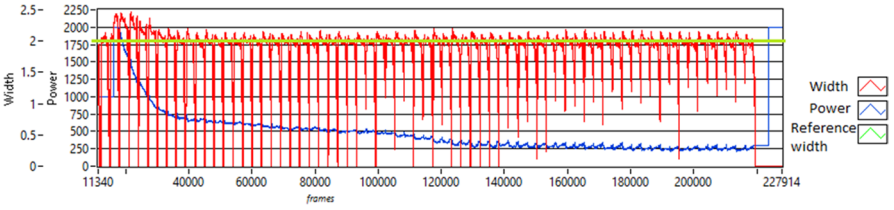

Fig. 11 Power and width graph for sample 3 (CLAMIR controlled)

Geometrical Feature Analysis

The geometric consistency is one of the most important features for any deposition. Visual inspection shows a similar trend for walls fabricated with and without CALMIR (Fig. 8). It is interesting to note that in both samples unidirectional scan strategy was employed. i.e., laser was kept on only on the start of the layer and was switched off on return. The use of closed loop control/manual power reduction does not show any substantial effect in keeping the geometry of wall.

When constant power mode was used with the same number of layers the wall only reached in height almost half as compared to controlled power (for both manual power reduction mode and for CLAMIR controlled) even though all the other parameters were kept constant. This phenomenon is well discussed in literature. With constant power for the initial layers more and more heat gets dissipated through the substrate. But as the layer advances more radial heat dissipation start to occur and hence the outwards velocity of melt pool flow increases due to outward Marangoni's Effect [27]. This causes an uneven width of the layers and in this case an increase of clad width which caused a decrease of overall wall height. Also, gradually the layers were seen to be bent through the middle. Due to this effect gradual reduction of laser power is advised by many researchers [6, 10, 28, 29]. By manually reducing power by 100 W with each successive layer (Fig. 9(b)) an overall geometric consistency like ClAMIR controlled samples (Fig. 12) was achieved.

However, from table of results (Table 4) it is evident that the width in case of manual power reduction could not be controlled with much precision, in fact, the width increased with height having a maximum value of 3.2 mm (Fig. 10).

The clad width in case of closed-loop control (CLAMIR) with bidirectional scan strategy was constant and the wall height was also like what was predicted. Figure 12 shows these fabricated samples. When the melt pool width was forced to be controlled at 2 mm via CLAMIR the width of clad decreases with wall height. The un-melted powder was seen to be stuck to the wall Fig. 12 (a). The reason is that on inspection of CLAMIR data it was found that to keep the melt

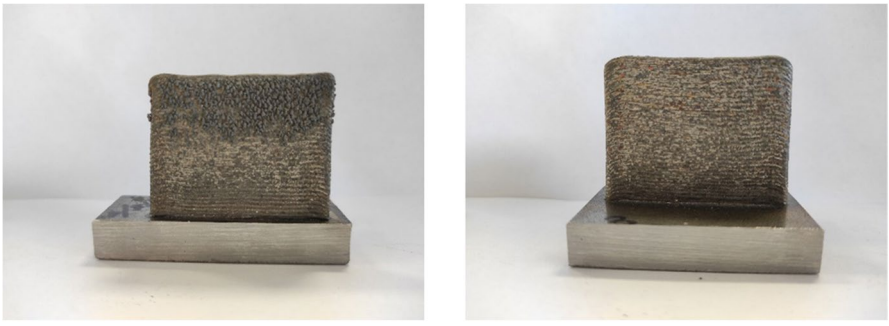

Fig. 12 **(a)** Sample 4 (with CLAMIR) and **(b)** Sample 5 (with CLAMIR)—Bidirectional Scan Strategy

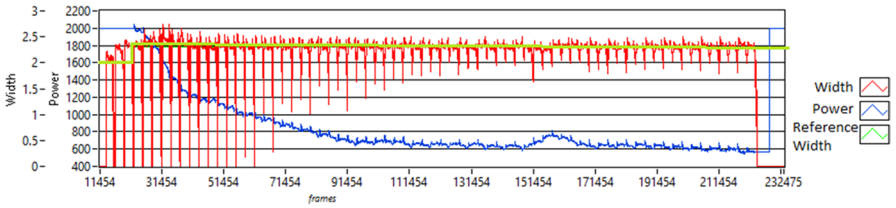

Fig. 13 Power and width graph of sample 5 (CLAMIR controlled)

pool width at 2 mm the laser power was reduced to almost 250 W. The graph from CALMIR data supports this as shown in Fig. 11.

This reduction occurred gradually but since the powder feed rate was constant therefore this low laser power was unable to melt enough powder. Thus, a system coupled with close loop control for power as well as for feed rate adjustment would bring a near ideal system. This is also the reason of reduced clad width for the top-most layers where the powder is seen to be stuck to the outer surface of the wall.

The CALMIR was set to auto calculate the melt pool during the first three layers and then implement the control from the fourth layer in case of sample 5. A good geometric consistency for both the clad widths, over all height and uniform clad length was achieved. Since the melt pool width depends greatly on laser power and powder feed rate, therefore, when control was operated from system given values, better results were seen. The obtained graph for sample 5 is given in Fig. 13. The auto calculation of width for sample 5 for the first three layers, reveals that the reference width changes from 2 mm to 2.31 mm which can be

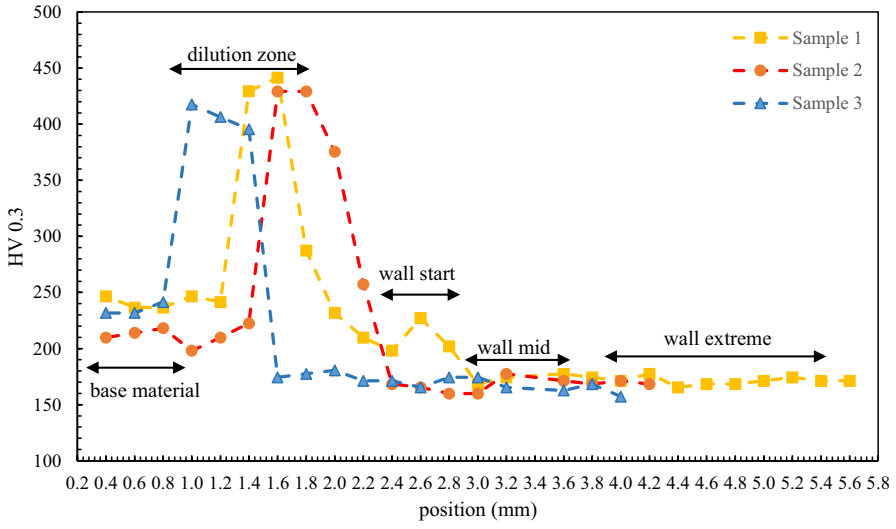

Fig. 14 Microhardness for samples without closed loop control

seen in graph from Fig. 13 and then CLAMIR uses this reference width to control the power till the end of fabrication.

Microhardness Analysis

The microhardness measurements were taken for substrate, dilution zone (depth of melt pool below the substrate level) and the wall for all the samples. Vickers Microhardness with 300 g load for a dwell time of 15 s was used. Since wall was also cut into half therefore the position (mm) mentioned in graphs was combined for all the three areas (wall start, mid and extreme) and therefore depicts only the increments between successive indents for each of three, but when combined this distance does not reflect the exact position of indent on the wall. For example, for sample 1 the position (mm) value is 5.6 mm but in fact it is showing the extreme end of the wall which reached a height of 17 mm as from Table 4. The three areas are therefore mentioned in the graphs for each of the samples. In all the cases regardless of closed loop control the hardness value was found to be high for dilution zone. Microhardness decreased as the wall progresses in height. The first layers also had higher values due to the dilution between 316L and the low carbon steel substrate as also shown by the Abdalla R. Nassar [9]. The middle layers of the wall had low values of hardness as compared to both start and the top layers. This attribute is typical for DED fabricated parts due to cyclic thermal history as the heat build-up in middle layers is higher as compared to both first and last layers. Due to this reason the central layers have less micro hardness values compared to first and last layers of DED fabricated parts [30]. This trend is most visible for sample 4 shown in Fig. 15. The graph for the hardness values for samples fabricated without closed loop control and with manual power reduction mode is shown in Fig. 14. The graph in Fig. 15

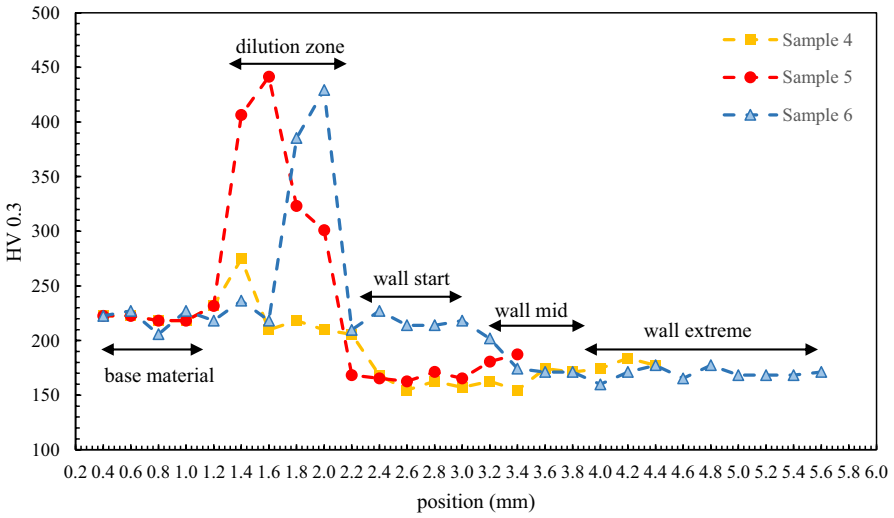

Fig. 15 Microhardness for samples with closed loop control

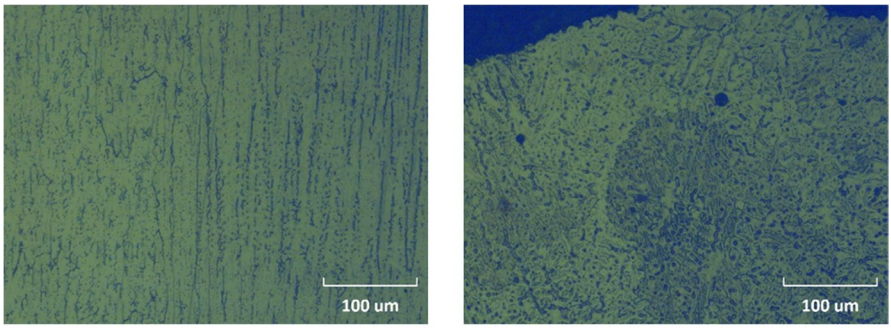

Fig. 16 Microstructure for Sample 1 **(a)** 1st Layers and **(b)** Last Layers

represents the microhardness values for samples fabricated via closed loop control. There was a scatter in the values within the three defined areas. Since sometimes the indent might be placed just on the interface between the two layers that returned higher values. This was evident after the etching of the samples with higher scatter values. In all the cases the laser power had a significant effect on the hardness values. Upon analysing samples which were geometrically inconsistent it was found that the microhardness values were lower as compared to the other samples. Since in this case the section was taken when the layer just started towards its length. While all the other samples were cut through the middle. This shows that the hardness values change along the height as well as along the layer length. This could be due to the different temperature gradient along the laser scan direction as compared to the temperature gradient along the height of thin wall as also demonstrated by the Wang et. al. [31]

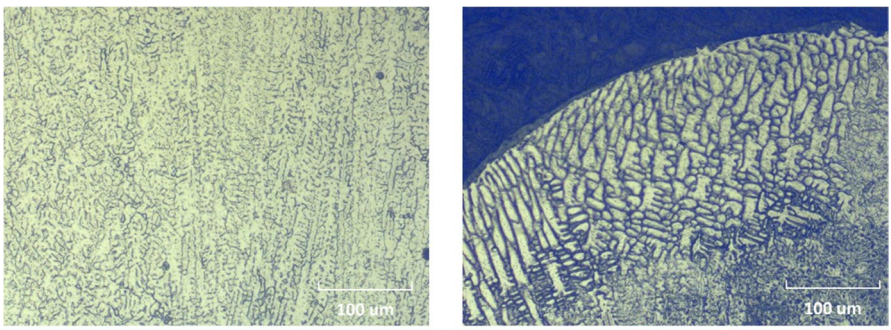

Fig. 17 Microstructure for Sample 4 **(a)** first layers **(b)** last layers

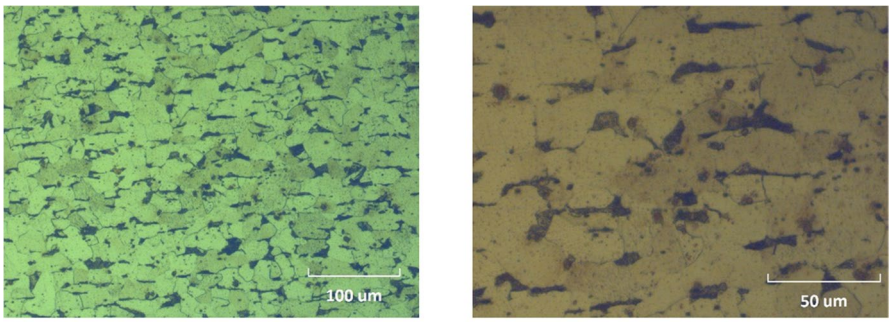

Fig. 18 Microstructure of base material **(a)** 4 × magnification **(b)** 5 × magnification

Porosity Analysis

The images of polished samples taken from Microscope were evaluated for density analysis by using ImageJ software by conversion to binary images. Overall, it was found that samples with excellent density were fabricated in case of all the samples. This attributed to the feasibility of process parameters for fabrication of such thin-walled structures. The highest density was recorded for the sample#1 (fabricated via constant power). The constant laser power induces almost fully dense part but compromised the geometrical features of the wall. The density results obtained for each sample are reported in Table 4. The porosity increased upon using closed loop control yet managed to fabricate thin wall with good geometrical features. This increase of porosity occurred due to the excessive reduction of laser power by closed loop control system.

Microstructure Analysis

The microstructure of DED manufactured parts cannot be predicted with much reliability due to complex thermal behaviour. Process parameters that influence the height cooling/heating rate, bulk temperature increment define the grain size

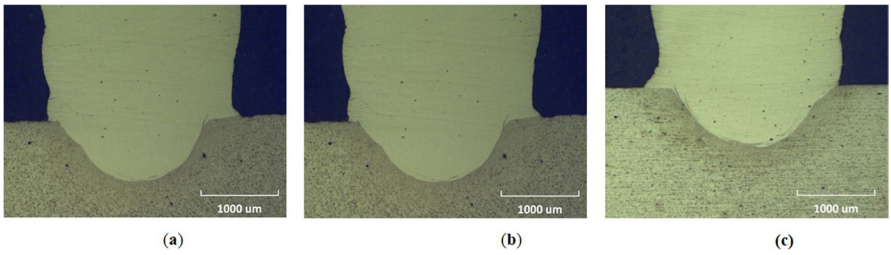

Fig. 19 Depth of melt pool below the substrate level **(a)** sample 1 **(b)** sample 2 **(c)** sample 3

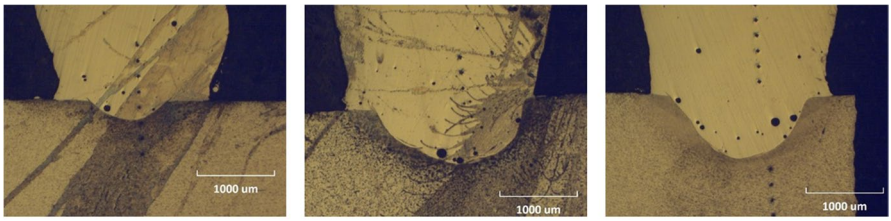

Fig. 20 Depth of melt pool below the substrate level **(a)** sample 4 **(b)** sample 5 **(c)** sample 6

and morphology of microstructure [32]. The microstructure of sample1 is shown in Fig. 16.

The microstructure for sample 4 for the 1st and the last layer is shown below in Fig. 17.

On comparison between the samples it can be seen that the microstuctre of samples represent the columnar dendritic structure. This is typical for parts manufatured via DED. The layers were found to be free from defects. The samples manufactured via close loop control somewhat represents a more homogenous microstructure as compared to the ones that were built with constant power. This could be due to the fact of better cooling condions due to gradual reduction of laser power. The microstructure reulted coincides with the work of Bi et al. Saboori et al. [33] also shows that the microstructre differs in the middle and edges of the meltpool. For overall part however, the microstructre grows with columar dendritic structute in direction of maximum thermal gradient dominates for the first and middle layers. For the last layers cellular structures are reported [33]. Figure 18 shows the microstructure of substrate. The images taken for the measurements of depth of melt pool below the substrate level are also given as reference (Fig. 19, Fig. 20).

To achieve a metallurgical bond a minimum amount of bonding is required between the subsequent layers which is quantified by using a dimensionless parameter called dilution. This attribute is more common where clad layers are deposited to improve the tribology of substrates such as corossion and wear. Nevertheless the dilution among the layers impacts the final microstructure due to subsequent melting and remelting of sucessive layers [34]. However in this study the penetration depth between the melt pool below the substrate level is reported. A stable bond between the substrate and the clad can be seen from the Fig. 19 and Fig. 20. The low penetration depth of melt pool into substrate for sample 4 could be explained with the extreme decrease of laser power that was commanded by CLAMIR to keep the melt pool at 2 mm width.

Conclusion

Thin-walled features (316L stainless steel) were successfully fabricated (S235JR substrate) by using two different scan strategies. These strategies were also tested with a closed loop control system that controls the melt pool width in real time.

The initial parameter window was selected based on the experience with processing of the similar materials. The following conclusions were drawn based on the results.

- Bidirectional scan strategy yields a geometrically consistent thin-walled features.
- Closed loop control system to control the melt pool cannot achieve a geometrically consistent part if the correct scan strategy is not chosen for the part to be built.
- Almost dense part with 99.78% density was fabricated with constant power, however, the density decreased in case of using CLAMIR and is recorded to be 99.40%.
- Real time control of melt pool width as a function of laser power can achieve parts that have better geometric features, however, at the expense of compromising the density. More pores were seen in case when the laser power was controlled by closed loop control system.
- Mechanical characterization shows that the micro hardness values range from 165–231 (HV0.3) and is not influenced by the closed loop control system even when it fed a low power of 600 W for the top layers.

Acknowledgements The author(s) kindly acknowledge the support of bi-rex: Big Data Innovation and Research Excellence (Bologna, Italy) and in particular engineer Mr. Lorenzo Ceccon and Ms Giulia Baglieri.

Funding Open access funding provided by Alma Mater Studiorum - Università di Bologna within the CRUI-CARE Agreement. This research did not receive any specific grant from funding agencies in the public, commercial, or not-for-profit sectors.

Availability of data and material The data that support the findings of this study are available on request from the corresponding author, [Nashit].

Code availability The code developed for the manufacturing are available upon request.

Declarations

Conflicts of interest The authors declare that they have no known competing financial interests or personal relationships that could have appeared to influence the work reported in this paper.

References

1. Fatoba, O.S.; Akinlabi, S.A.; Akinlabi, ;.E.T. ScienceDirect Laser Metal Deposition Influence on the Mechanical Properties of Steels and Stainless Steel Composites: A Review. **5**, 18603 (2018)
2. Dass, A.; Moridi, A. State of the Art in Directed Energy Deposition: From Additive Manufacturing to Materials Design. *Coatings (Basel)* **9**, 418 (2019) DOI https://doi.org/10.3390/coatings9070418. Available online: https://explore.openaire.eu/search/publication?articleId=dedup_wf_001::8197e6c7b2cf5087df9a88cd0dd02f88
3. Tang, Z.; Liu, W.; Wang, Y.; Saleheen, K.M.; Liu, Z.; Peng, S.; Zhang, Z.; Zhang, H. A review on in situ monitoring technology for directed energy deposition of metals. *International journal of advanced manufacturing technology* **108**, 3437–3463 (2020) DOI https://doi.org/10.1007/s00170-020-05569-3. Available online: https://search.proquest.com/docview/2419557964
4. KELL, J.; TYRER, J.R.; HIGGINSON, R.L.; THOMSON, R.C. Microstructural characterization of autogenous laser welds on 316L stainless steel using EBSD and EDS. *Journal of microscopy (Oxford)* **217**, 167–173 (2005) DOI https://doi.org/10.1111/j.1365-2818.2005.01447.x. Available online: https://onlinelibrary.wiley.com/doi/abs/https://doi.org/10.1111/j.1365-2818.2005.01447.x
5. Luzin, V.; Hoye, N. Stress in Thin Wall Structures Made by Layer Additive Manufacturing. *Residual Stresses 2016* (2016) DOI https://doi.org/10.21741/9781945291173-84
6. Pant, P.; Chatterjee, D.; Samanta, S.K.; Nandi, T.; Lohar, A.K. A bottom-up approach to experimentally investigate the deposition of austenitic stainless steel in laser direct metal deposition system. *Journal of the Brazilian Society of Mechanical Sciences and Engineering* **42** (2020) DOI https://doi.org/10.1007/s40430-019-2166-0. Available online: https://search.proquest.com/docview/2343270760
7. Choi, J., Chang, Y.: Characteristics of laser aided direct metal/material deposition process for tool steel. Int. J. Mach. Tools Manuf **45**, 597–607 (2005). https://doi.org/10.1016/j.ijmachtools.2004.08.014
8. Liu, J., Li, L.: Effects of process variables on laser direct formation of thin wall. Opt. Laser Technol. **39**, 231–236 (2007). https://doi.org/10.1016/j.optlastec.2005.08.012
9. El Cheikh, H.; Courant, B.; Branchu, S.; Huang, X.; Hascoët, J.; Guillén, R. Direct Laser Fabrication process with coaxial powder projection of 316L steel. Geometrical characteristics and microstructure characterization of wall structures. *Optics and lasers in engineering* **50**, 1779–1784 (2012). https://doi.org/10.1016/j.optlaseng.2012.07.002
10. Amine, T.; Newkirk, J.W.; Liou, F. An investigation of the effect of direct metal deposition parameters on the characteristics of the deposited layers. *Case studies in thermal engineering* **3**, 21–34 (2014) DOI https://doi.org/10.1016/j.csite.2014.02.002. Available online: https://explore.openaire.eu/search/publication?articleId=base_oa_____::42035c1040d04a19c3dba5f6ddfc508f
11. Zhang, K., Wang, S., Liu, W., Shang, X.: Characterization of stainless steel parts by Laser Metal Deposition Shaping. Materials in engineering **55**, 104–119 (2014). https://doi.org/10.1016/j.matdes.2013.09.006
12. Ya, W., Pathiraj, B., Liu, S.: 2D modelling of clad geometry and resulting thermal cycles during laser cladding. J. Mater. Process. Technol. **230**, 217–232 (2016). https://doi.org/10.1016/j.jmatprotec.2015.11.012
13. Peyre, P.; Aubry, P.; Fabbro, R.; Neveu, R.; Longuet, A. Analytical and numerical modelling of the direct metal deposition laser process. *Journal of physics. D, Applied physics* **41**, 025403 (2008) DOI https://doi.org/10.1088/0022-3727/41/2/025403. Available online: http://iopscience.iop.org/0022-3727/41/2/025403
14. Li, Y., Yang, H., Lin, X., Huang, W., Li, J., Zhou, Y.: The influences of processing parameters on forming characterizations during laser rapid forming. Mater. Sci. Eng., A **360**, 18 (2003). https://doi.org/10.1016/s0921-5093(03)00435-0
15. Amine, T.; Newkirk, J.; Liou, F. An investigation of the effect of laser deposition parameters on characteristics of multilayered 316 L deposits. *Int J Adv Manuf Technol* **73**, 1739–1749 (2014) DOI https://doi.org/10.1007/s00170-014-5951-z. Available online: https://search.proquest.com/docview/2262382970
16. Wang, H.; Liu, W.; Tang, Z.; Wang, Y.; Mei, X.; Saleheen, K.M.; Wang, Z.; Zhang, H. Review on adaptive control of laser-directed energy deposition. *Optical engineering* **59**, 070901 (2020) DOI https://doi.org/10.1117/1.OE.59.7.070901. Available online: http://www.dx.doi.org/https://doi.org/10.1117/1.OE.59.7.070901

17. Starr, T.L. In-Line Process Monitoring of Powder-Bed Fusion and Directed-Energy Deposition Processes. *Additive Manufacturing Processes* **287** (2020) DOI https://doi.org/10.31399/asm.hb.v24.a0006564
18. Izadi, M.; Farzaneh, A.; Mohammed, M.; Gibson, I.; Rolfe, B. A review of laser engineered net shaping (LENS) build and process parameters of metallic parts. , DOI https://doi.org/10.1108/RPJ-04-2018-0088
19. Moralejo, S.; Penaranda, X.; Nieto, S.; Barrios, A.; Arrizubieta, I.; Tabernero, I.; Figueras, J. A feedforward controller for tuning laser cladding melt pool geometry in real time. *Int J Adv Manuf Technol* **89**, 821–831 (2017) DOI https://doi.org/10.1007/s00170-016-9138-7. Available online: https://search.proquest.com/docview/1880771717
20. Ding, Y., Warton, J., Kovacevic, R.: Development of sensing and control system for robotized laser-based direct metal addition system. Addit. Manuf. **10**, 24–35 (2016). https://doi.org/10.1016/j.addma.2016.01.002
21. Akbari, M.; Kovacevic, R. Closed loop control of melt pool width in robotized laser powder–directed energy deposition process. *Int J Adv Manuf Technol* **104**, 2887–2898 (2019) DOI https://doi.org/10.1007/s00170-019-04195-y. Available online: https://search.proquest.com/docview/2267282072
22. Song, L.; Bagavath-Singh, V.; Dutta, B.; Mazumder, J. Control of melt pool temperature and deposition height during direct metal deposition process. *Int J Adv Manuf Technol* **58**, 247–256 (2011) DOI https://doi.org/10.1007/s00170-011-3395-2. Available online: https://link.springer.com/article/https://doi.org/10.1007/s00170-011-3395-2
23. Vandone, A., Baraldo, S., Valente, A., Mazzucato, F.: Vision-based melt pool monitoring system setup for additive manufacturing. Procedia CIRP **81**, 747–752 (2019). https://doi.org/10.1016/j.procir.2019.03.188
24. Ocylok, S., Alexeev, E., Mann, S., Weisheit, A., Wissenbach, K., Kelbassa, I.: Correlations of Melt Pool Geometry and Process Parameters During Laser Metal Deposition by Coaxial Process Monitoring. Phys. Procedia **56**, 228–238 (2014). https://doi.org/10.1016/j.phpro.2014.08.167
25. Errico, V.; Campanelli, S.L.; Angelastro, A.; Dassisti, M.; Mazzarisi, M.; Bonserio, C. Coaxial Monitoring of AISI 316L Thin Walls Fabricated by Direct Metal Laser Deposition. *Materials* **14**, 673 (2021) DOI https://doi.org/10.3390/ma14030673. Available online: https://www.ncbi.nlm.nih.gov/pubmed/33535644
26. Control for Laser Additive Manufacturing with Infrared Imaging User manual.
27. Han, L., Liou, F.W.: Numerical investigation of the influence of laser beam mode on melt pool. Int. J. Heat Mass Transf. **47**, 4385–4402 (2004). https://doi.org/10.1016/j.ijheatmasstransfer.2004.04.036
28. Wang, L., Felicelli, S.: Process Modeling in Laser Deposition of Multilayer SS410 Steel. J Manuf Sci Eng **129**, 1028–1034 (2007). https://doi.org/10.1115/1.2738962
29. Raghavan, A.; Wei, H.L.; Palmer, T.A.; Debroy, T.; Raghavan, A.; Wei, H.L.; Palmer, T.A.; Debroy, T. Citation. *Journal of Laser Applications* **25** (2013)
30. Thompson, S.M., Bian, L., Shamsaei, N., Yadollahi, A.: An overview of Direct Laser Deposition for additive manufacturing; Part I: Transport phenomena, modeling and diagnostics. Addit. Manuf. **8**, 36–62 (2015). https://doi.org/10.1016/j.addma.2015.07.001
31. Wang, L.; Felicelli, S.D.; Craig, J.E. 1.3173952. , DOI https://doi.org/10.1115/1.3173952
32. Saboori, A.; Aversa, A.; Marchese, G.; Biamino, S.; Lombardi, M.; Fino, P. Microstructure and Mechanical Properties of AISI 316L Produced by Directed Energy Deposition-Based Additive Manufacturing: A Review. *Applied sciences* **10**, 3310 (2020) DOI https://doi.org/10.3390/app10093310. Available online: https://search.proquest.com/docview/2403770770
33. Saboori, A., Aversa, A., Bosio, F., Bassini, E., Librera, E., De Chirico, M., Biamino, S., Ugues, D., Fino, P., Lombardi, M.: An investigation on the effect of powder recycling on the microstructure and mechanical properties of AISI 316L produced by Directed Energy Deposition. Materials science & engineering A, Structural materials : properties, microstructure and processing **766**, 138360 (2019). https://doi.org/10.1016/j.msea.2019.138360
34. Dass, A.; Moridi, A. State of the Art in Directed Energy Deposition: From Additive Manufacturing to Materials Design. *Coatings (Basel)* **9**, 418 (2019). https://doi.org/10.3390/coatings9070418. Available online: https://search.proquest.com/docview/2548331217